Deep-Sea Research II 94 (2013) 31–43

Contents lists available at ScienceDirect

Deep-Sea Research II

journal homepage: www.elsevier.com/locate/dsr2

Linkages between sea-ice coverage, pelagic–benthic coupling, and the distribution of spectacled eiders: Observations in March 2008, 2009 and 2010, northern Bering Sea

L.W. Cooper [a,*], M.G. Sexson [b], J.M. Grebmeier [a], R. Gradinger [c], C.W. Mordy [d], J.R. Lovvorn [e]

[a] Chesapeake Biological Laboratory, University of Maryland Center for Environmental Science, PO Box 38, Solomons, MD 20688, USA
[b] US Geological Survey, Alaska Science Center, 4210 University Drive, Anchorage, AK 99508, USA
[c] School of Fisheries and Ocean Science, University of Alaska Fairbanks, Fairbanks, AK 99775, USA
[d] Joint Institute for the Study of the Atmosphere and Ocean, University of Washington, 3737 Brooklyn Ave NE, Box 355672, Seattle, WA 98105-5672, USA
[e] Department of Zoology and Center for Ecology, Southern Illinois University, Carbondale, IL 62901, USA

ARTICLE INFO

Available online 7 March 2013

Keywords:
Bering Sea
Spectacled eider
Sea ice
Pelagic–benthic coupling
Organic sedimentation

ABSTRACT

Icebreaker-based sampling in the northern Bering Sea south of St. Lawrence Island in March of 2008, 2009, and 2010 has provided new data on overall ecosystem function early in the annual productive cycle. While water-column chlorophyll concentrations (<25 mg m^{-2} integrated over the whole water column) are two orders of magnitude lower than observed during the spring bloom in May, sea-ice algal inventories of chlorophyll are high (up to 1 g m^{-3} in the bottom 2-cm of sea-ice). Vertical fluxes of chlorophyll as measured in sediment traps were between 0.3 and 3.7 mg m^{-2} d^{-1} and were consistent with the recent deposition (days' to weeks' time scale) of chlorophyll to the surface sediments (0–25 mg m^{-2} present at 0–1 cm). Sediment oxygen respiration rates were lower than previous measurements that followed the spring bloom, but were highest in areas of known high benthic biomass. Early spring release of sedimentary ammonium occurs, particularly southeast of St. Lawrence Island, leading to bottom-water ammonium concentrations of >5 μM. These data, together with other physical, biological, and nutrient data, are presented here in conjunction with observed sea-ice dynamics and the distribution of an apex predator, the Spectacled Eider (*Somateria fischeri*). Sea-ice dynamics in addition to benthic food availability, as determined by sedimentation processes, play a role in the distribution of spectacled eiders, which cannot always access the greatest biomass of their preferred bivalve prey. Overall, the data and observations indicate that the northern Bering Sea is biologically active in late winter, but with strong atmospheric and hydrographic controls. These controls pre-determine nutrient and chlorophyll distributions, water-column mixing, as well as pelagic–benthic coupling.

1. Introduction

The northern Bering Sea, which we define as the continental shelf north of St. Matthew Island extending to the Bering Strait, is a large-scale ecotone between the pelagic-dominated southeast Bering Sea and more Arctic waters found north of the Bering Strait. In the region around St. Lawrence Island (SLI), nutrient distributions are controlled by the course and extent of the Anadyr Current (AC) from the western side of the Bering Sea (reviewed by Cooper et al., 2012). The AC has its origin in the deep Bering Sea and consists of waters that upwell onto the Bering shelf from the Bering Slope Current (Kinder et al., 1975; Wang et al., 2009). A branch of the AC passes south of SLI, although the main flow is northward through Anadyr Strait (Clement et al., 2005; Danielson et al., 2006, 2011; Grebmeier and Cooper, 1995).

To the east of SLI, the Bering Sea is dominated by Alaska Coastal Water (ACW), which is nutrient-poor compared to the AC to the west. Prior to the initiation of seasonal biological production, however, the contrast in nutrient concentration across the northern Bering Sea is smaller than observed during the open water season when a drawdown occurs due to biological productivity. In summer, generally nutrient-poor runoff from rivers in Alaska also creates a west-to-east gradient of decreasing salinity across the northern Bering Sea.

The alignment of high productivity by water mass and the shallow shelf of the Bering Sea result in a large proportion of high-quality organic carbon being deposited to the continental shelf, which in turn supports highly productive benthic communities (reviewed by Grebmeier, 2012; Grebmeier et al., 2006). Benthic communities in turn support apex predators such as the Pacific

* Corresponding author. Tel.: +1 410 326 7359; fax: +1 410 326 7341.
E-mail address: cooper@umces.edu (L.W. Cooper).

0967-0645/$ - see front matter © 2013 Elsevier Ltd. All rights reserved.
http://dx.doi.org/10.1016/j.dsr2.2013.03.009

Walrus (*Odobenus rosmarus divergens*), Bearded Seal (*Erignathus barbatus*), Gray Whale (*Eschrichtius robustus*), several sea duck species (Subfamily Merginae), and other organisms that forage on benthic food sources. Despite high benthic biomass and evidence for recent ecosystem-scale declines in biomass and shifts in biological community structure (Grebmeier, 2012), there has been limited sampling in this region during periods of ice cover (e.g. Clement et al., 2004; Cooper et al., 2002, 2012; Danielson et al., 2006), which is typically present from November until May or June. Information regarding ecosystem dynamics in the northern Bering Sea during the late winter period (March) is critical for understanding the initiation of the productive biological spring bloom as solar radiation increases sufficiently to initiate biological production. However, opportunities to document pre-seasonal conditions have been limited by seasonal (e.g., sea ice and extreme cold temperatures) and logistical (e.g., icebreaker-based instrumentation) constraints.

We present observations of hydrographic and biological conditions present on three research cruises in March 2008, March 2009, and March 2010. Specifically, we present mapped water mass boundaries (derived from salinity, oxygen isotopes and inorganic nutrients), water column nutrients and chlorophyll, the vertical flux of sea ice algal and phytoplankton pigments, and an inventory of recently deposited chlorophyll (days to weeks) on the sea floor.

We discuss measured physical and biogeochemical processes, particularly organic sedimentation that drives high benthic biomass in the context of a case study of the distribution of one apex predator that uses this region, the Spectacled Eider (*Somateria fischeri*). While our study was not focused on benthic community structure and dynamics, we use known distributions of benthic invertebrates as a means to explore the interplay between sea ice coverage, benthic invertebrate distribution, and the distribution of eiders.

Spectacled eiders are medium-sized sea ducks (spring adults: 1275–1850 g) that nest in coastal areas of northern and western Alaska, and northern Russia, yet spend most of the annual cycle at non-breeding (i.e., fall molting, wintering, and spring staging) areas in the near-shore East Siberian, Chukchi, Beaufort, and northern Bering Seas (Petersen et al., 2000). As a result of rapid population decline (up to 96% from 1952 to 1993) within the western Alaska breeding population, the species was designated 'threatened' under the US Endangered Species Act in 1993 (Ely et al., 1994; Stehn et al., 1993; US Fish and Wildlife Service, 1993). Subsequently, critical habitat was designated throughout the species' range, including an area encompassing the primary wintering site in the northern Bering Sea south of SLI (73,530 km^2; US Fish and Wildlife Service, 2001).

2. Methods

A suite of samples were collected and observations made during two cruises of the USCGC *Healy* (Cruise 08-01, 13–26 March 2008 and Cruise 09-01, 10–31 March 2009) and one cruise of the USCGC *Polar Sea* (Cruise 10-01, 7 March–7 April 2010) while sea ice was continuing to form under late winter conditions (Tables 1–3). A majority of sampling stations had been previously occupied for water column and benthic biological studies dating back to 1990 and earlier. Other stations were selected in situ to document localized water column conditions and prey available to spectacled eiders and Pacific walruses observed at the time of the cruise. Data relevant to the distribution of spectacled eiders are presented here; Pacific walrus data are in preparation (C. Jay, personal communication).

The conductivity, temperature, and depth (CTD) instrument used aboard both *Healy* and *Polar Sea* consisted of a 12-place rosette with 30-L Niskin bottles and a Sea-Bird Electronics Model 911+ CTD system. Salinities were standardized with a Guideline Autosal salinometer with international seawater standards. The electronics system was calibrated before and after the cruises at the Sea-Bird manufacturing facility in Bellevue, Washington. Niskin bottles were closed at selected depths during the up-cast, usually 0, 10, 20, 30, 40 and 50 m below the surface and a final bottle closed at 5–10 m above the sea floor (bottom water) as determined by an altimeter installed on the CTD.

Table 1
HLY0801 station information.

Station number	Station name	Date (m/dd/yyyy)	Latitude °N	Longitude °W	Depth (m)
1	VNG1	3/16/2008	61.974	−175.050	79
2	NWC5	3/16/2008	62.048	−175.201	80
3	NWC4	3/17/2008	62.381	−174.567	72
4	VNG3.5	3/17/2008	62.568	−173.579	68
5	SWC2	3/17/2008	62.915	−172.298	60
6	NWC2.5	3/18/2008	63.033	−173.446	70
7	NWC3	3/18/2008	62.799	−173.929	70
8	NWC4a	3/18/2008	62.578	−174.165	70
9	DLN3	3/19/2008	62.879	−174.538	72
10	NWC2	3/19/2008	63.119	−173.122	71
11	POP3a	3/20/2008	62.550	−172.320	60
12	SIL3	3/20/2008	62.438	−172.300	60
13	SEC2.5	3/20/2008	62.483	−171.848	60
14	POP4	3/21/2008	62.400	−172.705	60
15	FD1	3/21/2008	62.482	−172.464	55
16	SEC2	3/21/2008	62.601	−170.968	45
17	NEC2	3/21/2008	62.424	−170.113	39
18	WAL1	3/21/2008	62.387	−169.362	33
19	WAL2	3/22/2008	62.394	−169.381	36
20	WAL3	3/22/2008	62.367	−168.976	36
21	WAL4	3/22/2008	62.562	−169.318	34
22	WAL5	3/22/2008	62.522	−169.635	30
23	WAL6	3/22/2008	62.404	−169.720	34
24	MK10A	3/23/2008	62.192	−169.010	36
25	NEC1	3/23/2008	62.754	−169.594	42
26	JGR1	3/23/2008	62.711	−170.167	43
27	SEC1	3/23/2008	62.992	−170.289	40
28	JGR2	3/23/2008	62.988	−170.800	40
29	JGR3	3/23/2008	63.158	−170.921	37
30	JGR4	3/23/2008	63.116	−171.301	46

The stable oxygen isotope composition of water samples was also measured in surface water samples to assess freshwater contributions from runoff relative to melted sea ice. Isotopic analyses were performed via equilibration with carbon dioxide within a Thermo Delta Plus Gas Bench and stable isotope mass spectrometer used in a continuous flow mode at the University of Maryland Center for Environmental Science with internal and international standards used for calibration. Data are reported for oxygen isotopes of these surface waters, as well as carbon isotopes of marine algal sediment trap samples (methodology described below), in the delta notation, where

$$\delta X = [(R_{sample}/R_{standard})-1] \times 1000$$

where X is ^{18}O or ^{13}C of the sample and R is the corresponding ratio $^{18}O/^{16}O$ or $^{13}C/^{12}C$. Analytical precision was ±0.1‰.

Nutrient samples were collected from all CTD casts during the cruise and analyzed for nitrate, nitrite, ammonium, phosphate and silicate. Samples were collected in a 60-ml syringe after three complete seawater rinses, and filtered through a 45-μm cellulose acetate membrane directly into acid washed 25-ml high-density polyethylene bottles rinsed three times with unfiltered seawater. Samples were then frozen at −80 °C until analyzed. Nutrient analysis was carried out at the Pacific Marine Environmental Laboratory (PMEL) following the protocols of Gordon et al. (1994), including reagent preparation, equipment calibration, preparation of primary and secondary standards, and corrections for

Table 2
HLY0901 station information.

Station number	Station name	Date (m/dd/yyyy)	Latitude °N	Longitude °W	Depth (m)
1	VNG1	3/14/2009	62.016	−175.071	79
2	NWC5	3/14/2009	62.055	−175.197	80
3	NWC4	3/14/2009	62.381	−174.536	71
4	SWC3	3/15/2009	62.558	−173.087	62
5	NWC2.5A	3/16/2009	62.970	−173.384	71
6	DLN2	3/16/2009	63.278	−173.737	74
7	NWC2	3/17/2009	63.104	−173.146	70
8	NWC1	3/17/2009	63.487	−172.317	50
9	VNG3.5	3/18/2009	62.566	−173.568	67
	VNG3.5	3/18/2009	62.563	−173.559	67
10	SIL2	3/19/2009	62.762	−171.654	50
11	SEC2	3/19/2009	62.590	−170.962	45
12	CD2	3/20/2009	62.530	−172.122	51
13	SEC1.5	3/20/2009	62.812	−170.645	45
14	NEC1	3/21/2009	62.758	−169.586	42
15	SEC1	3/21/2009	62.986	−170.266	40
16	SIL1	3/21/2009	63.100	−171.295	47
17	JGR3	3/21/2009	63.160	−170.941	40
18	WAL7	3/22/2009	62.743	−169.316	38
19	WAL8	3/22/2009	62.627	−169.636	40
20	WAL9	3/22/2009	62.668	−169.140	40
21	MK1	3/22/2009	62.728	−168.951	40
22	WAL10	3/23/2009	62.521	−168.970	33
23	WAL11	3/23/2009	62.255	−169.638	40
24	WAL12	3/24/2009	62.067	−169.272	40
25	XSL1	3/24/2009	62.073	−169.762	40
26	XSL2	3/24/2009	62.068	−170.252	45
27	NEC3	3/24/2009	62.067	−170.621	50
28	XSL3	3/24/2009	62.046	−171.118	50
29	SLP1	3/24/2009	62.374	−170.371	41
30	SLP1A	3/25/2009	62.493	−170.482	40
31	SLP2	3/25/2009	62.631	−170.502	42
32	SLP3	3/25/2009	62.870	−170.634	43
33	JGR3	3/25/2009	63.156	−170.918	40
34	SEC1	3/25/2009	62.977	−170.270	40
35	NEC1	3/25/2009	62.754	−169.589	40
36	MK1B	3/25/2009	62.725	−169.017	36
37	WALI13	3/26/2009	62.859	−169.016	35
38	SEC1.5	3/27/2009	62.811	−170.648	43
39	SIL2.5	3/27/2009	62.632	−171.991	50
40	CD1	3/27/2009	62.676	−173.372	70
41	NWC3	3/27/2009	62.760	−173.816	72
42	POP4	3/28/2009	62.388	−172.700	60
43	SWC4A	3/28/2009	62.239	−173.741	60

blanks and refractive index. Silicate analysis was conducted a second time at least 1 day after thawing to minimize complications due to polymerization (Macdonald et al., 1986).

During the two *Healy* cruises, water column chlorophyll *a* was measured by filtering 250-mL water samples through 25-mm GF/F filters. The filters were initially frozen (~1 h) to fracture cell walls, and then stored in 10 mL of 90% acetone at 4 °C for 24 h in the dark. This storage temperature was used because it is close to in situ water temperatures and presumably results in low rates of chlorophyll degradation. Chlorophyll *a* was extracted and measured using the Welschmeyer (1994) method with a Turner Designs 10-AU field fluorometer. The fluorometer was calibrated with a Turner Design Part no. 10-850 chlorophyll standard before and after all sampling, with the use of a secondary solid standard (Part no. 10-AU-904) during sampling to identify any possible instrument drift. Integrated chlorophyll *a* was calculated for individual stations from ocean surface to sediments on a square meter basis, as most stations were 40–60 m in depth.

A similar procedure was used during the *Polar Sea* cruise to measure chlorophyll *a*. In addition, replicate samples were collected, filtered onto 25-mm GF/F filters, placed into 1.5-mL microcentrifuge tubes and stored at −80 °C, and returned frozen to PMEL for post-cruise analysis. Filters were stored in 10 mL of 90% acetone at 4 °C for 24 h in the dark, and then analyzed on a Turner Designs 10-AU field fluorometer using the Welschmeyer method. Replicates were collected to evaluate of the impacts of freezing and storing the filters prior to measuring chlorophyll.

Ice sampling occurred in 2009 and 2010 at stations (Table 4) selected according to ice and weather conditions, and overall cruise planning. Sampling occurred during daytime around solar noon on ice floes considered representative for a given area. We sampled ice floes of sufficient thickness for safe field work (>0.25 m), whereas new ice (e.g. pancake, grease, nilas) was not sampled.

Ice cores were taken with a 9-cm diameter ice corer. Cores were sectioned into 1 to 20-cm long segments and stored in coolers in the dark for transport. Core segments were melted directly in a dark and cold room (2–4 °C) and split into 5 to 250-ml subsamples. One subsample was filtered onto Whatman GF/F filters, and frozen for algal pigment analysis. A second subsample was filtered onto pre-combusted GF/F filters to later analyze the stable isotope composition (δ^{13}C, δ^{15}N) of organic material and quantify particulate organic carbon and nitrogen (POC, PON; data to be presented elsewhere). Filters for algal pigment analysis were extracted with 7 ml of 90% acetone for 24 h (Gradinger et al., 2005) and analysis was conducted fluorometrically with a Turner Designs fluorometer (Arar and Collins, 1997).

Filters containing organic matter were dried 1–2 d and HCl-fumed to remove carbonates. Filters were analyzed at the University of Alaska Fairbanks Stable Isotope Facility using an elemental analyzer coupled to a Thermo Delta stable isotope mass spectrometer operated in a continuous flow mode. Organic carbon isotope ratios are expressed in the conventional delta notation as described previously for oxygen isotope composition of surface waters.

An ice saw was used to cut holes in the ice, through which sediment traps were deployed for 2–6 h below ice floes at depths of 5 and 20 m. Traps were filled with 0.7-μm filtered seawater prior to deployment. Upon recovery, samples were parsed and treated using the same methods used to process ice samples. Live macroorganisms were manually removed from all samples.

Sediment samples (0–1 cm) were collected on all cruises for assessment of chlorophyll *a* surface sediment, as well as other sediment characteristics (e.g. total organic carbon, C:N ratios, grain size) reported elsewhere. Sediment samples were collected using a multi- or single-HAPS benthic corer (133 cm^2; Kanneworff and Nicolaisen, 1973) or from the top of a van Veen grab (0.1 m^2). In prior studies we determined that bioturbation is high on a month–annual scale and the less disturbed nature of surface sediments collected by corers relative to grabs is negated for these shelf sediments (Cooper et al., 1998; Pirtle-Levy et al., 2009). We also assumed that the 0–1 cm sediment depth increment predominantly contained chlorophyll deposited on a week–month time scale, based on the findings that surface sediment chlorophyll inventories in the northern Bering Sea vary in response to seasonally variable primary production in the ice and water column (Cooper et al., 2002).

Duplicate sediment cores for shipboard incubations were collected using a HAPS benthic corer with removable Plexiglas® insert sleeves (133-cm^2 surface area as described above). Under optimal conditions, the resultant cores were approximately 15-cm deep, with a low degree of apparent disturbance. Apparent disturbance was determined to be low if clear water was present at the sediment–water interface, flocculent materials such as fecal pellets were present at the base of benthic burrows at the sediment surface, and filtering activity was exhibited by macrobenthic invertebrates. Sediment–flux measurements for dissolved oxygen followed the methods of Grebmeier and McRoy (1989). Bottom water for these experiments was collected from the CTD

Table 3
Polar Sea 10-01 station information.

Station number	Station name	Date (m/dd/yyyy)	Latitude °N	Longitude °W	Depth (m)
1	VNG1	3/13/2010	62.018	−175.050	83
2	NWC5	3/13/2010	62.051	−175.200	84
2	NWC5	3/13/2010	62.047	−175.196	84
3	NWC4	3/14/2010	62.401	−174.527	74
4	NWC4A	3/15/2010	62.562	−174.210	73
5	VNG3	3/15/2010	62.555	−173.841	71
6	VNG35	3/16/2010	62.577	−173.624	70
7	CD1	3/16/2010	62.676	−173.367	70
8	VNG4	3/16/2010	62.756	−173.410	78
8	VNG4	3/16/2010	62.762	−173.435	71
9	NWC2.5	3/17/2010	63.033	−173.423	75
10	VNG5	3/17/2010	62.968	−172.986	70
11	SWC3A	3/17/2010	62.762	−172.710	65
12	POP3A	3/18/2010	62.576	−172.310	85
13	SIL3	3/18/2010	62.442	−172.312	55
14	SEC2.5	3/18/2010	62.496	−171.853	50
15	CD2	3/18/2010	62.531	−172.119	50
15	CD2	3/18/2010	62.560	−172.179	50
16	CD08	3/19/2010	62.653	−172.236	56
17	SIL2	3/19/2010	62.751	−171.664	50
18	SIL2.5	3/19/2010	62.630	−171.987	50
19	CD10C	3/20/2010	62.371	−172.383	56
20	CD10B	3/20/2010	62.258	−172.282	56
21	CD10A	3/20/2010	62.151	−172.178	55
22	SEC4	3/20/2010	61.924	−172.218	60
23	SEC3	3/20/2010	62.281	−171.563	52
24	NEC3	3/21/2010	62.059	−170.650	55
25	MK11	3/21/2010	62.178	−169.465	40
26	NEC2	3/21/2010	62.429	−170.057	40
27	NEC1	3/22/2010	62.759	−169.592	44
28	NEC1.1	3/22/2010	62.853	−169.887	46
29	NEC1.2	3/22/2010	62.648	−170.314	45
30	SEC2	3/22/2010	62.606	−170.955	47
31	SEC1.8	3/22/2010	62.692	−170.764	46
32	SEC1.5	3/23/2010	62.809	−170.646	45
33	SEC1.1	3/23/2010	62.887	−170.431	45
34	SEC1	3/23/2010	62.993	−170.267	42
35	CDF	3/23/2010	62.934	−170.928	46
36	CDF1.4	3/23/2010	62.860	−171.030	47
37	CD10D	3/23/2010	62.614	−171.385	50
38	POP4	3/24/2010	62.399	−172.686	46
39	SWC4	3/24/2010	62.226	−173.768	46
39	SWC4	3/24/2010	62.224	−173.776	65
40	SWC4A	3/25/2010	62.418	−173.411	65
41	NWC3	3/26/2010	62.748	−173.871	74
42	DLN3	3/26/2010	62.894	−174.515	80
43	DLN2	3/27/2010	63.264	−173.735	82
44	CD81.1	3/27/2010	62.632	−172.266	55
45	CD81.5	3/28/2010	62.719	−171.839	54
46	SWC2	3/28/2010	62.908	−172.275	60
47	NWC2	3/28/2010	63.131	−173.123	72
48	CDF	3/29/2010	62.920	−170.947	46
49	70M58	3/30/2010	62.199	−174.752	79
50	70M56	3/21/2010	61.950	−174.372	77
51	70M55	3/21/2010	61.860	−174.102	77
52	70M54	3/21/2010	61.738	−173.874	77
53	70M52	3/21/2010	61.419	−173.734	79
54	70M50	3/21/2010	61.074	−173.843	84
55	70M48	4/1/2010	60.749	−173.670	76
56	70M47	4/1/2010	60.571	−173.633	72
57	70M46	4/1/2010	60.429	−173.593	70
58	70M45	4/1/2010	60.265	−173.531	73
59	70M44	4/1/2010	60.101	−173.297	75
60	70M43	4/1/2010	60.042	−173.004	71
61	70M42	4/1/2010	59.962	−172.723	73
62	70M41	4/2/2010	59.911	−172.436	78
63	70M40	4/2/2010	59.904	−172.203	76
64	70M39	4/2/2010	59.884	−171.655	76
65	70M38	4/2/2010	59.779	−171.428	77
66	70M37	4/2/2010	59.709	−171.137	76
67	70M36	4/2/2010	59.591	−170.917	75
68	70M35	4/2/2010	59.450	−170.915	76
69	70M34	4/2/2010	59.335	−170.648	73
70	70M32	4/3/2010	59.113	−170.260	70
71	70M30	4/3/2010	58.789	−170.301	75

Table 3 (*continued*)

Station number	Station name	Date (m/dd/yyyy)	Latitude °N	Longitude °W	Depth (m)
72	70M28	4/3/2010	58.449	−170.153	77
73	70M26	4/3/2010	58.146	−169.917	77
74	70M24	4/3/2010	57.918	−169.512	73
75	70M22	4/3/2010	57.848	−168.899	75
76	70M20	4/4/2010	57.614	−168.729	74
77	70M17	4/4/2010	57.505	−168.009	75
78	70M14	4/4/2010	57.520	−167.049	75
79	70M11	4/4/2010	57.328	−166.351	74
80	70M08	4/4/2010	57.110	−165.611	75
81	70M04	4/5/2010	56.796	−164.582	77

Table 4
Sea ice sampling stations, 2009–2010.

Cruise	Station	Date (m/dd/yy)	Latitude °N	Longitude °W	Ice thickness (cm)	Snow depth (cm)
HLY0901	DLN2	3/16/09	63.267	−173.695	86	15
HLY0901	NWC1	3/17/09	63.485	−172.317	65	25
HLY0901	SEC2	3/19/09	62.594	−170.959	95	24
HLY0901	MK1	3/22/09	62.729	−168.952	87	14
HLY0901	WAL12	3/23/09	62.112	−169.256	67	16
HLY0901	MK1B	3/25/09	62.699	−169.024	68	34
HLY0901	NWC3	3/27/09	62.682	−173.388	109	33
PSea1001	NWC5	3/13/10	62.050	−175.199	53	3
PSea1001	VNG4	3/16/10	62.756	−173.411	53	2
PSea1001	CD2	3/18/10	62.532	−172.121	49	3
PSea1001	SWC4	3/24/10	62.225	−173.770	57	7
PSea1001	NWC3	3/25/10	62.754	−173.854	56	7
PSea1001	DLN2	3/26/10	63.263	−173.736	55.5	5
PSea1001	NWC2	3/28/10	63.131	−173.123	41.5	5

rosette. Enclosed sediment cores with motorized paddles were maintained in the dark at in situ bottom temperatures for approximately 12–24 h. Point measurements were made at the start and end of the experiment, and flux measurements were calculated, based on the concentration differences adjusted to a daily flux per m^2. Previous shipboard measurements indicated a steady decline in oxygen values in the overlying water during the course of incubation. Sediments were sieved after completing the experiment to determine faunal composition (data to be reported elsewhere).

Surface sediment chlorophyll *a* inventories were measured on all cruises using a Turner Designs fluorometer without acidification (Welschmeyer method) using a standardized method that includes a 12 h dark incubation in 90% acetone at 4 °C (Cooper et al., 2002). Surface sediment inventories reported are the mean of two independent determinations.

Satellite telemetry was used to collect weekly geo-referenced locations from adult and juvenile spectacled eiders. In 2008–2010, spectacled eiders were captured at coastal sites in western and northern Alaska. A veterinarian implanted a satellite transmitter (Model PTT 100, Microwave Telemetry Inc.) in the coelom of 92 individuals using standard surgical methods (Korschgen et al., 1996; Mulcahy and Esler, 1999). Permits for eider capture and transmitter deployment were obtained from the US Fish and Wildlife Service and the Alaska Department of Fish and Game, with capture and surgical protocols reviewed and approved by the USGS Alaska Science Center and the University of Alaska Fairbanks animal care and use committees. Satellite transmitters were programmed to provide location data every 4–7 days over a 2-year period. Location, body temperature, and voltage data were received from each transmitter through the Collecte Localisation Satellites Argos system (CLS America, Lanham, Maryland). Prior to analysis, we excluded location data from dead individuals and other poor quality data locations. The Douglas Argos-Filter Algorithm and associated software (Douglas, 2010) was used to synthesize multiple locations into the single most likely location received from each individual during each transmission period. Near-real time locations were used during research cruises in 2009 and 2010 to guide aerial surveys for spectacled eiders and document sea ice conditions in used areas.

We assessed general spatiotemporal patterns in the distribution of spectacled eiders at the species' primary wintering area, south of St. Lawrence Island in the northern Bering Sea, constraining analysis to an area south of 63°47'N and between 175° and 168° W. Within the primary wintering area, we assessed overlap in the distribution of spectacled eiders in September–May between 2008 and 2009, 2009 and 2010, and 2010 and 2011. We also compared all locations from winters 2008–2011 to similar telemetry data collected in 1993–1997 (Petersen et al., 1999). We used Geospatial Modeling Environment (Version 0.6.0.0, Beyer, 2012) to calculate kernel densities and 50% and 95% isopleths for each set of locations, using least squares cross-validation to calculate kernel smoothing parameters. We used ArcMap 10 (ArcGIS, ESRI, Redlands, CA) to calculate the percent overlap of paired isopleths (ESRI, 2010). We also used ArcMap to extract depth values at each location in the data set using the General Bathymetric Chart of the Oceans (The GEBCO_08 Grid, version 20100927, http://www.gebco.net).

Density of major bivalve prey of eiders at each sampling station was mapped based on van Veen grab samples taken in March–April 2001 and May–June 2006. Benthic samples collected contemporaneously with the eider telemetry data were being analyzed at the time of manuscript preparation. However, we expect more recently collected data will not fundamentally alter our understanding of where benthic biomass is greatest; see Grebmeier (2012) for a more detailed description of long-term changes in benthic community composition southwest of SLI. Furthermore, bivalves must be several years old to reach size classes considered preferred for eiders (Lovvorn et al., 2003). Therefore, we assumed that the dispersion of these prey in 2009 resembled dispersion in 2006. Maps of prey density were overlain

with maps of percent ice cover (in tenths) on 2 March 2001 and 2009, the same months in which eiders were collected for body condition and diet studies (J. Lovvorn, unpublished data). Ice cover percentages were derived from National Ice Center digital Ice Analysis charts, which are based on data sources (and spatial resolution) including RADARSAT 2 (100 m), ASAR (150 m), ENVISAT GMM (1 km), MODIS (0.25–1 km), AVHRR (1.1–2.9 km), and OLS (0.5–2.4 km).

3. Results and discussion

3.1. Hydrography, nutrients and chlorophyll fields

During our early spring observations in the northern Bering Sea in 2008, 2009, and 2010, the water column was highly mixed, partly a result of brine rejection (i.e. exclusion of salt from ice during sea ice formation). Temperatures were isothermal and near the freezing point (−1.8 °C) although salinity varied spatially if not vertically. Horizontal gradients in bottom salinity were generally the result of brine rejection south of SLI relative to less saline water present to the south and west (Fig. 1). This pattern differed from that observed during open-water seasons with salinity greater (>32.5) in the west (i.e. Anadyr water) and declining significantly to the east (<31) (e.g. Walsh et al., 1989). Some distinctions in water masses were observed based on the nutrient concentration. At this early point in the seasonal cycle, there was limited runoff in the Alaska coastal water to the east of SLI. For example, the stable oxygen isotope data (Fig. 2), as well as salinity (Fig. 1) showed negligible runoff relative to published early summer data (e.g. Cooper et al., 1997). Therefore, we concluded that salinity variation is primarily driven at this time by the

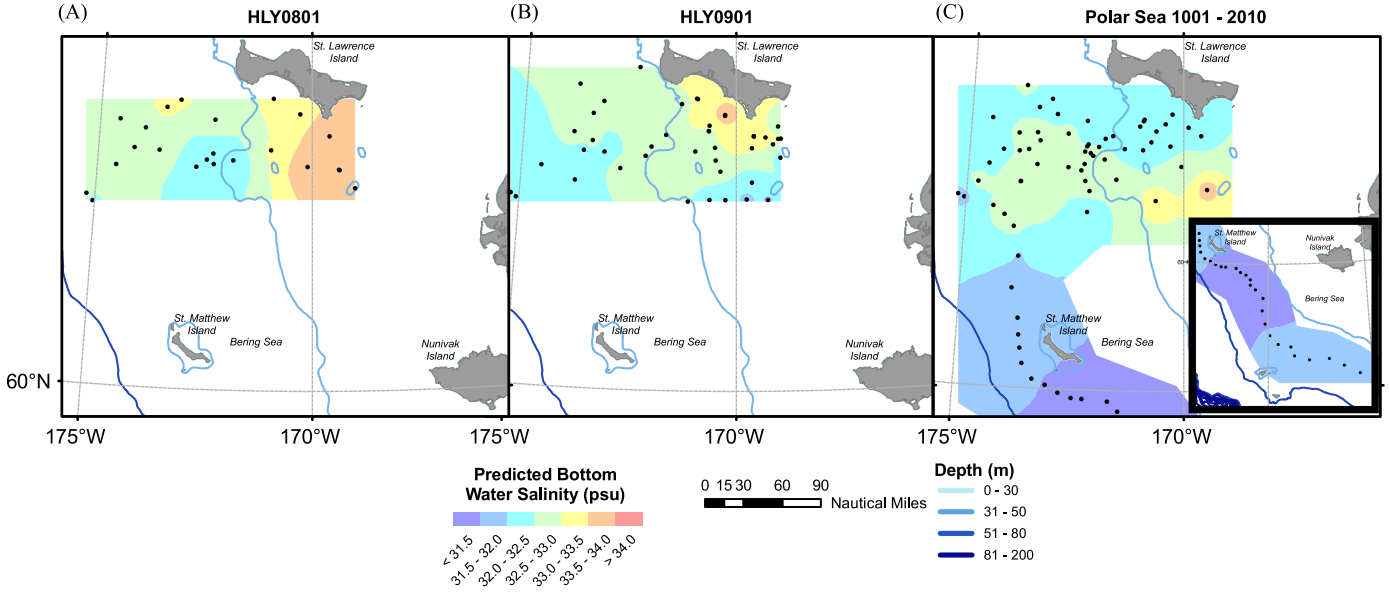

Fig. 1. Bottom water salinity in March 2008 (A), March 2009 (B) and March 2010 (C) south of St. Lawrence Island. Symbols correspond to the available data; color gradations are estimated (predicted) interpolations and are created using inverse distance weighting method (default settings) of Geospatial Analyst Extension for ArcMap 9.3 (ESRI, Redlands, CA) (For interpretation of the references to color in this figure legend, the reader is referred to the web version of this article.).

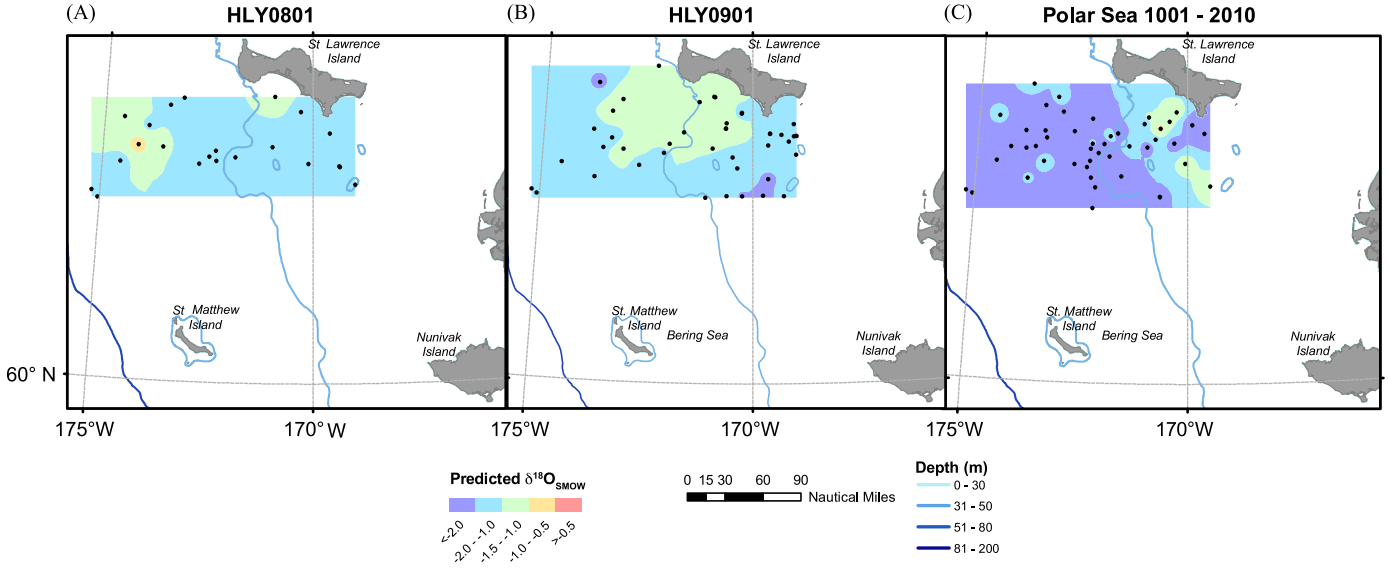

Fig. 2. Surface water $\delta^{18}O$ values in March 2008 (A), March 2009 (B) and March 2010 (C) south of St. Lawrence Island. Symbols correspond to the available data; color gradations are estimated interpolations using inverse distance weighting method (default settings) of Geospatial Analyst Extension for ArcMap 9.3 (ESRI, Redlands, CA). (For interpretation of the references to color in this figure legend, the reader is referred to the web version of this article.)

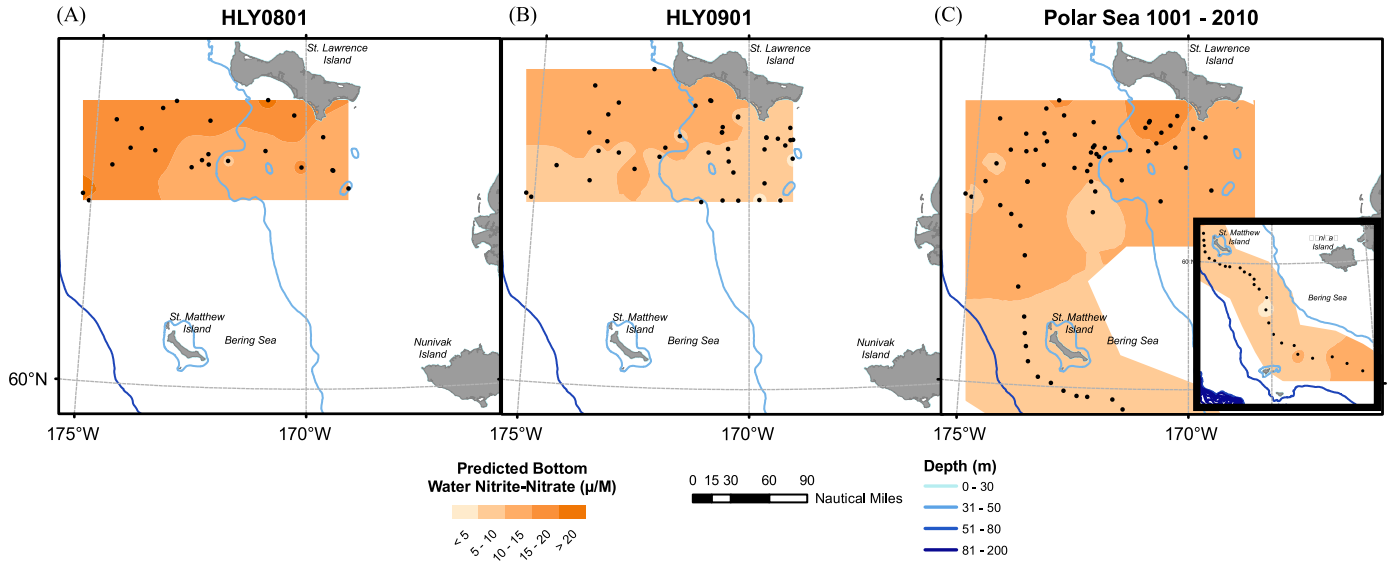

Fig. 3. Bottom water nitrate+nitrite (μM) in March 2008 (A), March 2009 (B) and March 2010 (C) south of St. Lawrence Island. Symbols correspond to the available data; color gradations are estimated interpolations as in Fig. 1. (For interpretation of the references to color in this figure legend, the reader is referred to the web version of this article.)

injection or rejection of brine from sea ice rather than differences between Anadyr water and Alaska coastal water. The greatest salinities were observed south and southeast of the island, resulting from brine rejected waters originating from the formation of sea ice in the polynya south of SLI (e.g. Fig. 1B). More saline waters were then advected south and apparently entrained into northeasterly flowing water on the Bering Shelf, as described in Danielson et al. (2006) and Cooper et al. (2012) (Fig. 1A and C). We also observed an elevation of $\delta^{18}O$ values in surface waters south of SLI to ~0.5% to −1.0% (an enrichment of ~1%, see Fig. 2), particularly in 2009 and 2010. Enrichments do not mirror salinity variations (Fig. 1) driven by water mass. Therefore, we think the pattern in oxygen isotope variability indicated the presence of a small freshwater component originating from melted sea ice. Freshwater is isotopically heavier (~2%) than the seawater from which it forms due to isotopic fractionation during ice formation. This suggests that at early stages of sea ice formation, such as when frazil or grease ice forms in the polynya south of SLI, some of the newly formed ice may subsequently pass back into a liquid phase, releasing a freshwater fraction isotopically more enriched in ^{18}O than other surface waters. Therefore, at early stages of sea ice formation, or in regions of active sea ice formation, there may be an isotopic signal present in surface waters that traces recent sea ice formation. To our knowledge, these patterns of isotopic enrichment of ^{18}O in surface waters in a polynya have not been reported previously.

Well-documented differences in water masses in the northern Bering Sea (e.g. Walsh et al., 1989) were apparent according to nutrient concentrations. A west-to-east decrease in bottom water nitrate+nitrite was unambiguously observed in 2 of the 3 years (Fig. 3A and B). In 2010, the greatest bottom water nitrate+nitrite concentrations (>20 μM) were observed immediately south of SLI, which may actually reflect a branch of the AC that flows south of the island (Danielson et al., 2006; Grebmeier and Cooper, 1995). However, placement of sampling stations in 2010 may have precluded clear mapping of the east-to-west increasing concentrations of nitrate+nitrite due to the influence of Anadyr water. Surface water concentrations of nitrate+nitrite were equally as high as bottom waters (data not shown) indicating biological production had not significantly impacted inorganic nutrients at this point in the seasonal cycle. Silica and phosphate varied in a similar spatial pattern as nitrate+nitrite (data not shown), meaning water mass differences in nutrients were present early in the season, but differences among water masses were not as great as observed following extensive water column production later in the season.

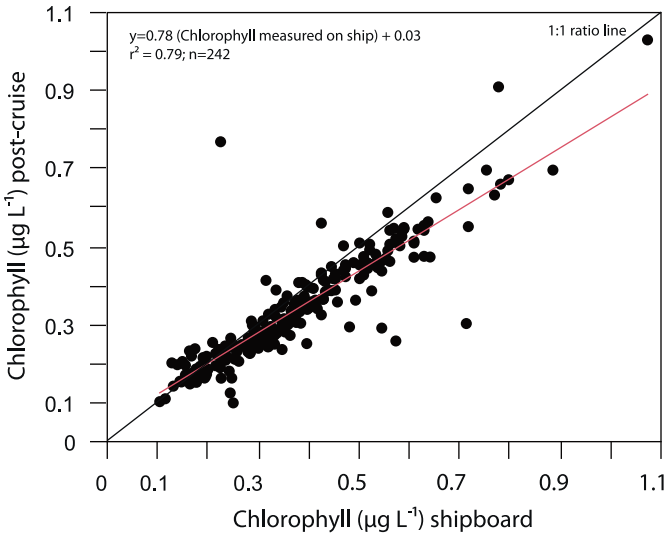

Fig. 4. Chlorophyll *a* concentrations in replicate water samples collected and analyzed during the Polar Sea 10–01 cruise (*x*-axis) versus frozen filters analyzed post-cruise (*y*-axis). The black regression line shows the expected 1:1 ratio for replicate samples. The red line shows the actual regression between the two sets of samples, indicating that chlorophyll *a* concentration determined shipboard, was on average 19% greater than replicate samples analyzed post-cruise from frozen filters. (For interpretation of the references to color in this figure legend, the reader is referred to the web version of this article.)

Systematic differences were observed between chlorophyll *a* measured shipboard and using frozen filters analyzed later (Fig. 4). Chlorophyll *a* concentrations determined shipboard using the Welschmeyer method shortly after sampling were on average ~19% greater than concentrations reported for samples from the same rosette bottles determined in the lab from frozen filters, otherwise using the same methods. This suggests degradation influenced the concentration of chlorophyll stored on frozen filters. Therefore, we used the shipboard chlorophyll determinations in our data analysis. However, further work is needed to assess the relative importance of various sources of chlorophyll degradation on frozen filters measured post-cruise (e.g. time until acetone extraction, storage temperature, etc.).

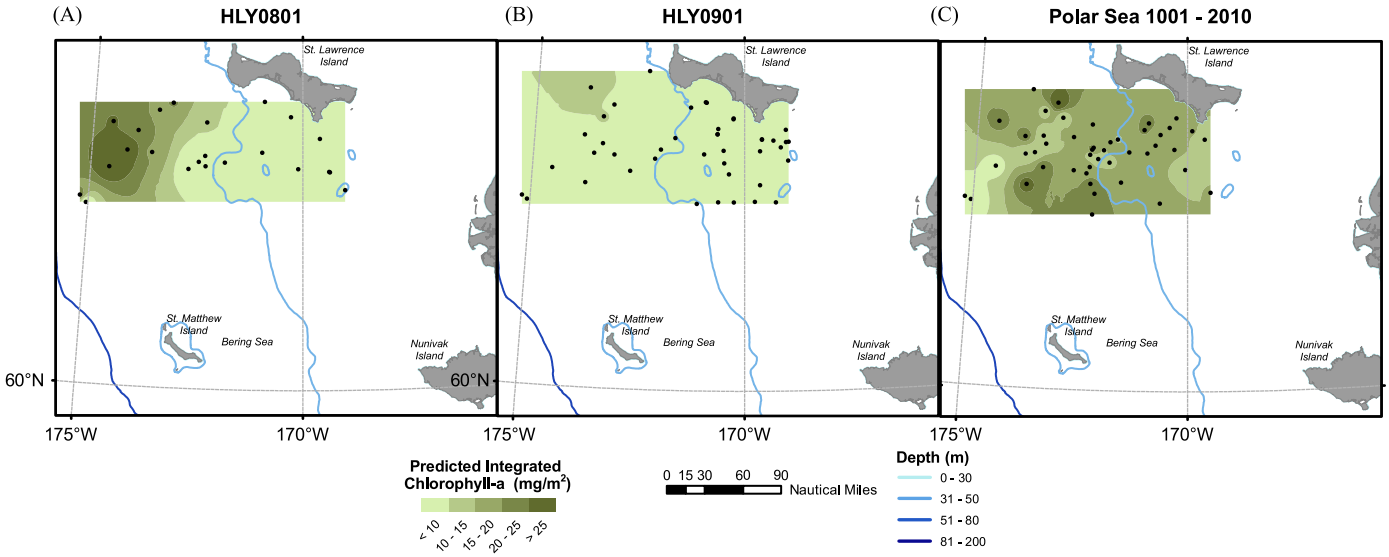

Fig. 5. Integrated chlorophyll *a* inventories (mg m^{-2}) in March 2008 (A), March 2009 (B) and March 2010 (C) south of St. Lawrence Island. The integrated chlorophyll *a* inventories are based on bottle measurements of chlorophyll *a* concentrations at discrete depths, which were summed from surface to seafloor. Symbols correspond to the available data; color gradations are estimated are estimated interpolations as in Fig. 1. (For interpretation of the references to color in this figure legend, the reader is referred to the web version of this article.)

Concentrations of chlorophyll *a* in the water column were integrated over the entire water column (Fig. 5). The higher integrated chlorophyll inventories tend to match the nitrate+nitrite bottom water concentrations driven by water mass (Fig. 3), although there was more complexity apparent in 2010 (Fig. 3C). In 2008 and 2009, a decreasing trend in integrated water column chlorophyll *a* was observed from west to east. The maximum integrated chlorophyll values (~25 mg chlorophyll *a* m^{-2}, or on volume basis: 0.5 mg m^{-3}) are consistent with previous measurements made in this region of the Bering Sea in April 1999 and March 2001 (Clement et al., 2004). However, these concentrations are also as much as two orders of magnitude lower than observations made during the peak of the spring bloom in May–June, with values of up to 1000 mg m^{-2} or more (Cooper et al., 2002, 2012). The sharp contrast in water column concentrations between March–April and May–June is clearly tied to sea ice break-up and rapid development of an ice-associated bloom. This ice edge initiated bloom includes sea ice obligate organisms such as pennate diatoms, but also cryophilic water column phytoplankton such as *Fragilariopsis* spp.

3.2. Sea ice measurements

Ice floe thickness in 2009 and 2010 varied between 42 and 109 cm and snow depth between 2 and 34 cm (Fig. 6A and B). Ice floes in 2009 were significantly ($p<0.001$, Mann–Whitney U-test) thicker than 2010 and covered with significantly ($p<0.001$, Mann–Whitney U-test) more snow. In both sea ice (bottom 1-cm) and the water column, algal pigment concentrations (Fig. 6C) were significantly greater in 2010 compared to 2009 ($p<0.001$, Mann–Whitney U-test), indicating thicker sea ice and snow in 2009 was associated with lower chlorophyll biomass. Overall sea ice chlorophyll concentrations significantly ($p<0.001$, Mann–Whitney U-test) exceeded phytoplankton values by about three orders of magnitude.

3.3. Sediment trap measurements

The vertical flux of chlorophyll *a* (Fig. 6E) varied between 0.3 and 3.7 mg chlorophyll *a* m^{-2} d^{-1} with a median value of 1.1 mg chlorophyll *a* m^{-2} d^{-1}. We did not observe a significant difference between years (Mann–Whitney U-test $p>0.8$) or between concentrations in the 5 and 20-m sediment traps (Mann–Whitney U-test, $p>0.8$). However, the $\delta^{13}C$ ratio (Fig. 6F) of the sinking material was significantly ($p<0.05$, Mann–Whitney U-test) more positive in 2010 compared to 2009 with an overall median value of −23.4‰. More positive $\delta^{13}C$ values in 2010 are consistent with greater light conditions under thinner ice and snow, greater photosynthetic rates, and reduced discrimination against ^{13}C during photosynthesis.

Observed export fluxes of chlorophyll *a* are similar in magnitude to observations from other first year ice regions in the Arctic (e.g. Michel et al., 2006) and are also consistent with inventories of chlorophyll in surface sediments during this early season sampling. Chlorophyll *a* extracted from surface sediments ranged from zero to upwards of 20 mg m^{-2} in each of the 3 years of the study (Fig. 7). In May–July, as primary production reaches a peak in the water column, more widely distributed and greater inventories in surface sediments are often observed (Cooper et al., 2002, 2012). Similarity, the order of magnitude of vertical fluxes (median of 1.1 mg m^{-2} d^{-1}) observed in the early season sampling compared with the inventory present in surface sediments (up to 20 mg m^{-2}) does not suggest steady-state conditions for deposition of chlorophyll to the surface sediments, but rather slow burial and/or consumption that occurs at a rate slower than sedimentation rates (see also discussion by Grebmeier and Barry, 2007).

3.4. Bottom water ammonium

Additional evidence of active early season biological activity included elevated ammonium concentrations observed in bottom water (Fig. 8) particularly in 2008 and 2009 to the southeast of SLI. Increased ammonium in bottom waters subsequent to spring production has been observed in other portions of the eastern Bering Sea shelf (Mordy et al., 2012; Whitledge et al., 1986). In 2010, this pattern of elevated ammonium in bottom waters southeast of SLI was not observed. However, extended sampling along the 70-m isobath (not sampled in 2008 and 2009) showed relatively high ammonium concentrations in bottom water further to the south and southeast. Areas of high ammonium concentrations were generally not located in mud dominated areas where high oxygen utilization by benthic macrofauna have been observed in the past (Grebmeier et al., 2006), implying the importance of bacterial processes involved

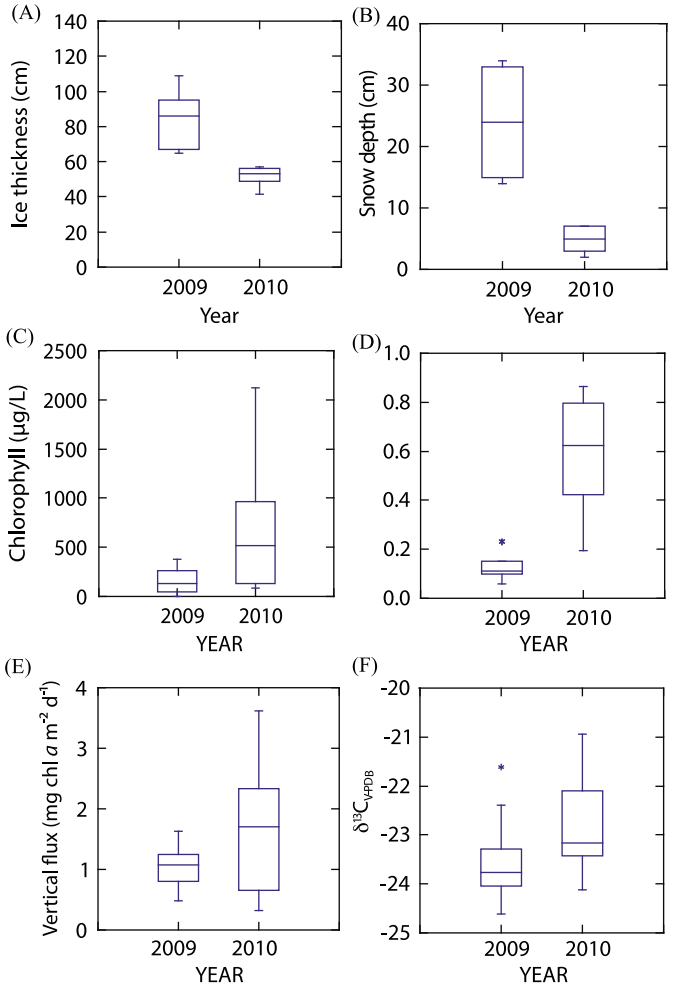

Fig. 6. (A) Sea ice thicknesses in 2009 and 2010 at sampled ice stations; (B) snow thickness on top of sea ice in 2009 and 2010 at sampled ice stations; (C) chlorophyll *a* concentrations in lowest 2 cm of sea ice in 2009 and 2010 at sampled ice stations; (D) chlorophyll *a* concentrations in water column in 2009 and 2010 at sampled ice stations; (E) vertical flux in chlorophyll *a* determined from short-term deployments of sediment traps anchored beneath the ice; (F) carbon isotope composition of organic matter collected in short-term sediment traps.

in regenerating inorganic nitrogen. Greater ammonium bottom water concentrations were also observed to the southeast of SLI where nitrate+nitrite tended to be lower (Fig. 3). Based on the expectations of slow southeastern movement of bottom waters away from SLI during sea ice formation (Danielson et al., 2006, 2011), bottom waters in contact with the sediments immediately south of the SLI may contribute ammonium and potentially regenerated nitrate through nitrification.

3.5. Sedimentation oxygen uptake

The rate of sediment oxygen uptake was as high as 16 mmol O_2 m^{-2} d^{-1}, centered on an area of high benthic biomass (described by Grebmeier, 2012; Grebmeier et al., 2006) to the southwest of SLI (Fig. 9). Rates of oxygen uptake rates were much lower than have been observed historically or at other times of year southwest of SLI (25–30 O_2 m^{-2} d^{-1}) when there is greater productivity in the water column (Cooper et al., 2012; Grebmeier, 2012; Grebmeier and Cooper, 1995; Grebmeier et al., 2006). The lower oxygen uptake rates we observed during this study are consistent with lower benthic biological activity prior to the peak of the bloom in May–June, but nevertheless indicate significant metabolic activity early in the season.

3.6. Spectacled eider distribution

Over winters 2008–2009, 2009–2010, and 2010–2011, we received 3229 high quality locations from tagged spectacled eiders within the primary wintering area (Fig. 10). Mean water depth at wintering locations was 42±13 m. Nearly all locations received during each winter originated from the primary wintering area, and concurrent aerial surveys and population estimates (approximately 380,000 individuals; W. Larned, personal communication) suggested that nearly the entire population of spectacled eiders winters in this area annually.

Eiders arrived at the wintering area as early as the last week of September and departed no later than the last week of May, constituting a maximum duration of approximately 9 months. Within each winter, we observed a complete spatiotemporal shift in the distribution of eiders. In general, eiders occupied an area approximately 45 km southwest of Southeast Cape on SLI in

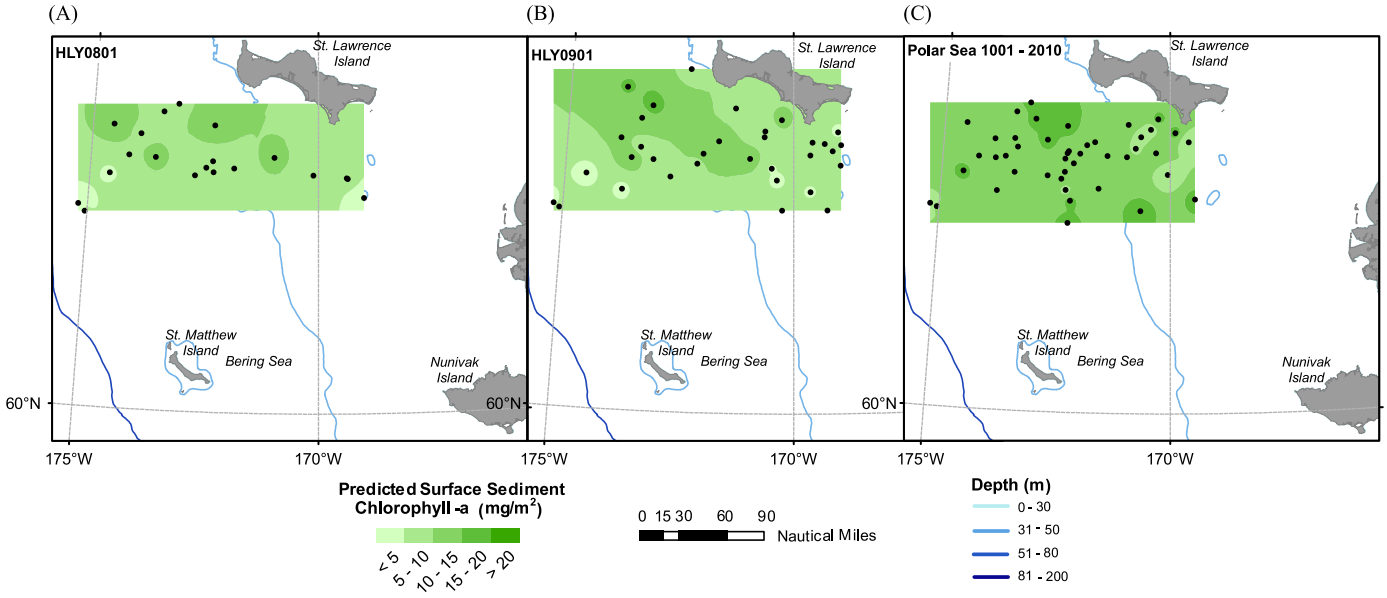

Fig. 7. Chlorophyll *a* inventories (mg m^{-2}) in surface (0–1 cm) sediments March 2008 (A), March 2009 (B) and March 2010 (C) south of St. Lawrence Island. Symbols correspond to the available data; color gradations are estimated are estimated interpolations as in Fig. 1. (For interpretation of the references to color in this figure legend, the reader is referred to the web version of this article.)

October–November. In December, eiders shifted to an area approximately 70 km to the west-southwest where most remained through April (Figs. 11A and 12A). The reasons for this shift are not understood; sea ice had not developed potentially forcing eiders to move, and benthic resources were likely not exhausted in the area used in early winter. However, the latter area is well matched with the greatest biomass of benthic bivalves (Grebmeier, 2012; Grebmeier et al., 2006), and among spectacled eiders collected in this area in 2001, almost 100% of esophageal contents were bivalve *Nuculana radiata* (Lovvorn et al., 2003).

Pair-wise percent overlap of 50% kernel isopleths between winters 2008 and 2009, 2009 and 2010, and 2010 and 2011 ranged from 16.9% to 58.5%, indicating interannual use of similar core wintering areas (Fig. 11A). Pair-wise percent overlap of 95% kernel isopleths ranged from 65.7% to 77.4%, indicating eiders generally used the same primary wintering area in all years (Fig. 12B). Within each winter, the distribution and location of eiders appeared to respond to sea ice concentration. Eider locations were more concentrated during periods of greater ice density. However, additional analysis is needed to quantify eider movement in response to the density and movement of ice.

Percent overlap of 50% and 95% kernel isopleths between winters 1993–1997 and 2008–2011 was 21.7% and 44.8%, respectively, indicating eiders generally used the same areas during each period (Fig. 12A and B). The 50% isopleth representing the distribution of eiders in December–April in 2008–2011 was approximately 50 km northeast of the distribution in 1993–1997, suggesting a possible shift in the late winter distribution of spectacled eiders in recent years. However, substantial differences in the number and quality of locations received during each period introduce considerable uncertainty to comparison between sampling periods.

Based on the previous models of foraging energetics, the average abundance of the preferred bivalve *Nuculana radiata* must exceed 90 m^{-2} for spectacled eiders to maintain positive energy balance throughout winter (Lovvorn et al., 2009). Near the site where eiders were collected on 19 March 2001, adequate prey

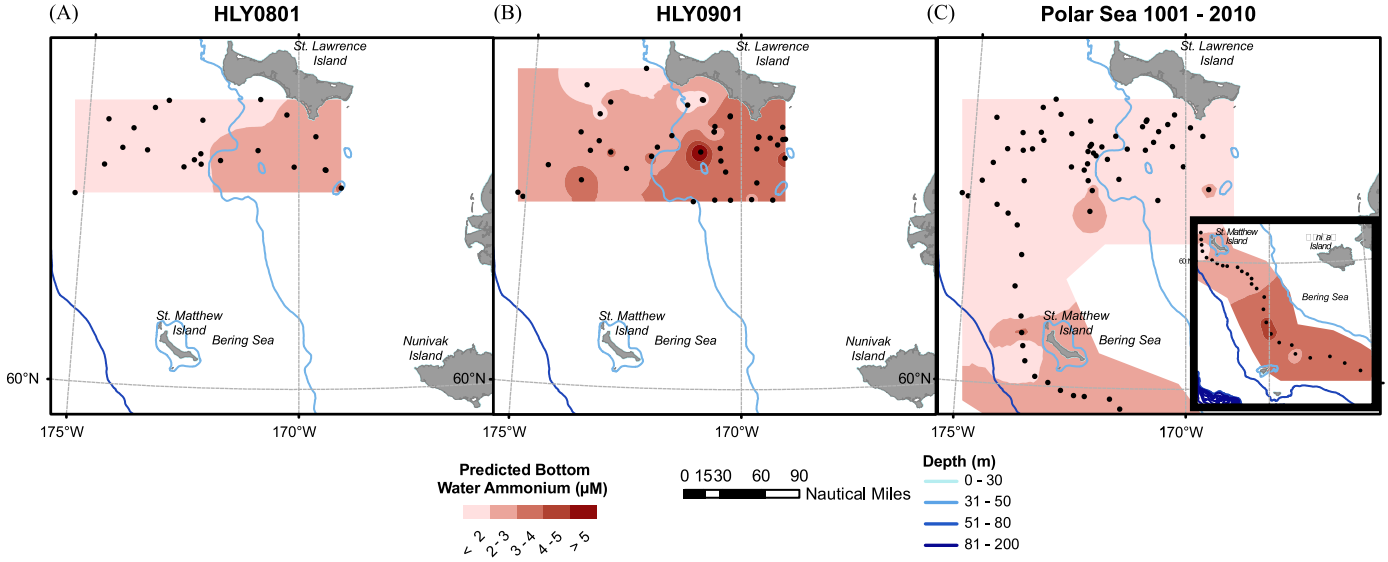

Fig. 8. Bottom water ammonium in March 2008 (A), March 2009 (B) and March 2010 (C) south of St. Lawrence Island. Symbols correspond to the available data; color gradations are estimated (predicted) interpolations and are estimated interpolations as in Fig. 1. (For interpretation of the references to color in this figure legend, the reader is referred to the web version of this article.)

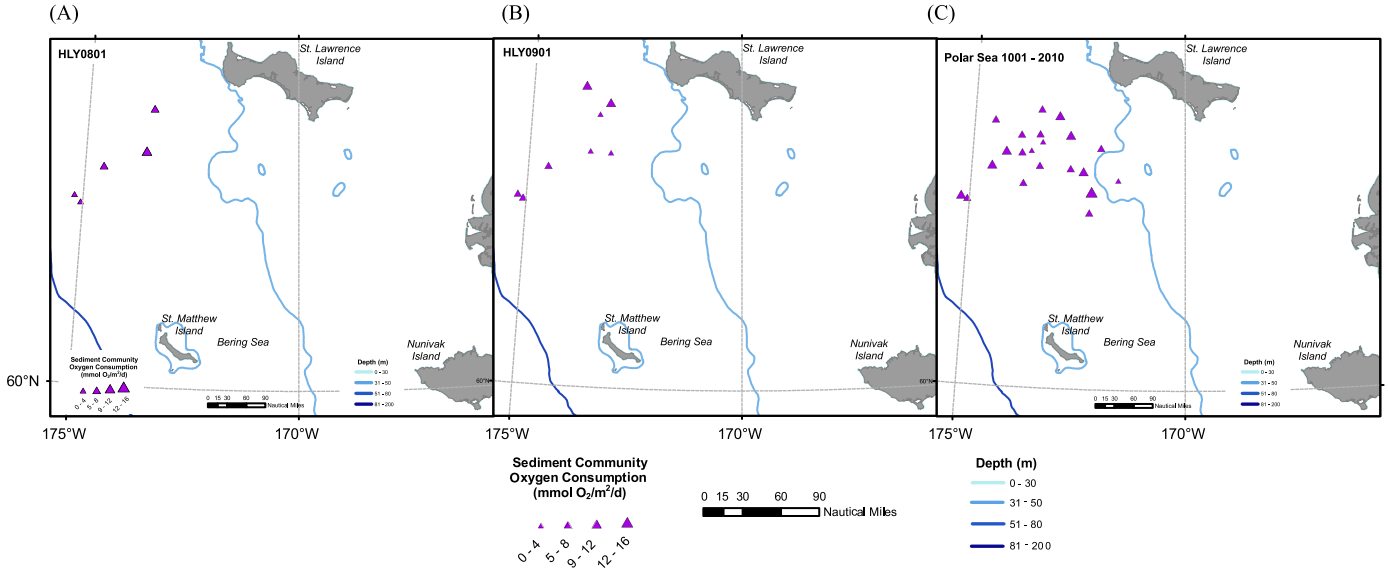

Fig. 9. Sediment oxygen consumption as measured in duplicate 133 cm^2 cores incubated shipboard for 12–24 h in March 2008 (A), March 2009 (B), and March 2010 (C). Symbols correspond to the available data; because of relatively limited sampling, no color interpolations are shown.

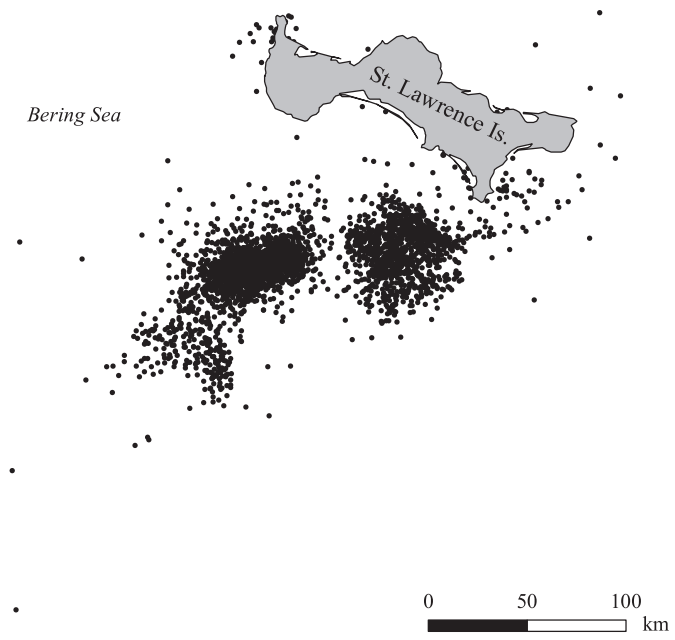

Fig. 10. Spectacled eider satellite telemetry locations ($n=3229$) received from the primary wintering area in the Bering Sea south of St. Lawrence Island, Alaska, in September–May in 2008–2009, 2009–2010, and 2010–2011.

densities were distributed mostly in a large contiguous region with many openings in the ice that allowed eiders access to those prey (Fig. 13). In contrast, areas with sufficient prey densities in 2009 were more scattered and covered with mostly continuous ice with few openings. Visual observations during helicopter surveys from 14 to 22 March 2009 revealed very few leads in the region where eiders had been collected on 19–22 March 2001. Near the collection site in 2009, leads were few, small, and contained very high densities of eiders, i.e., numbers of birds per spatial area of open-water. Further analyses revealed that severe ice conditions in 2009 had prevailed for most of winter. While benthic biomass and productivity in the northern Bering Sea are very well documented (e.g. Grebmeier, 2012; Grebmeier et al., 2006), our assessment of the interaction between eiders and benthic sources of prey should be treated with caution until benthic samples collected contemporaneously with the eider telemetry data (2009–2010) are fully analyzed (Grebmeier and Cooper, unpublished data). The major complexity is that while the distribution and overall biomass of the clam prey base are established, the size distribution varies annually, and spectacled eiders have specific size preferences (Lovvorn et al., 2003).

The fat content of spectacled eiders collected in late March was 33–35% lower in 2009 (Lovvorn, unpublished data) than in 2001, likely as a result of conditions in 2009 that were not encountered in 2001 namely thicker and more extensive ice that limited access to benthic foods. Female spectacled eiders lay eggs soon after arrival on

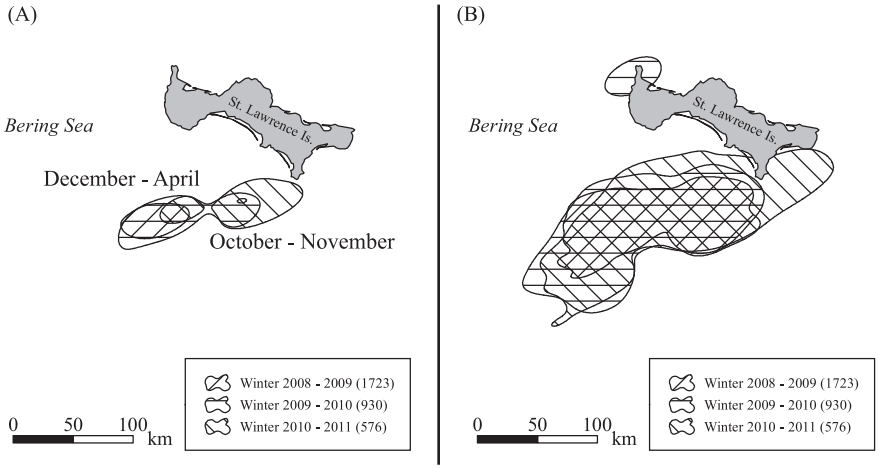

Fig. 11. Fifty percent (A) and 95% (B) kernel isopleths representing the distributional density of spectacled eider locations in the primary wintering area in the Bering Sea south of St. Lawrence Island, Alaska, in September–May in 2008–2009, 2009–2010, and 2010–2011. Samples sizes used to calculate each isopleth are in parentheses.

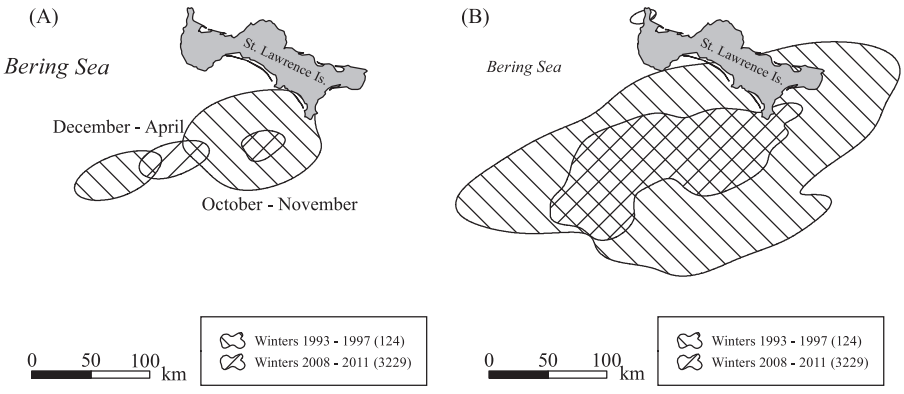

Fig. 12. Fifty percent (A) and 95% (B) kernel isopleths representing the distributional density of spectacled eider locations in the primary wintering area in the Bering Sea south of St. Lawrence Island, Alaska, in winters 1993–1997 and 2008–2011. Samples sizes used to calculate each isopleth are in parentheses.

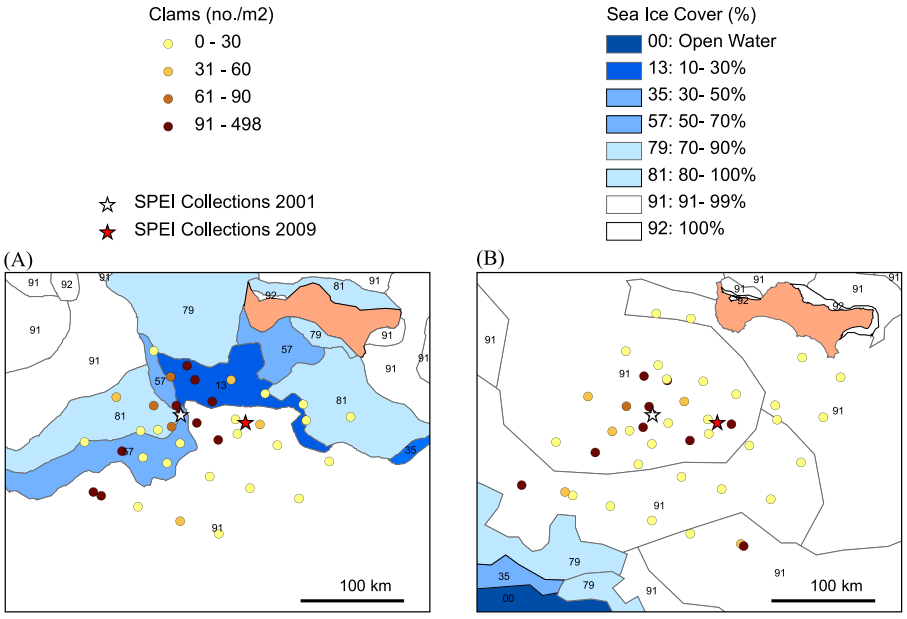

Fig. 13. Densities (number/m^2) of the primary prey of spectacled eiders (the bivalve *Nuculana radiata*) at sampling stations in (A) March–April 2001 and (B) May–June 2006, and the dispersion of percent ice cover on 2 March in (A) 2001 and (B) 2009, south of St. Lawrence Island in the Bering Sea. Collection sites for spectacled eiders on 19–22 March in 2001 (white stars) and 2009 (red stars) are shown. (For interpretation of the references to color in this figure legend, the reader is referred to the web version of this article.)

breeding areas in coastal Alaska and Russia, so females must carry enough stored nutrients to produce all eggs and accommodate loss of about 500 g of body mass by the end of incubation (Lovvorn et al., 2003; Petersen et al., 2000). Therefore, breeding propensity and/or success likely depend on stored reserves before arrival (Coulson, 1984; Oosterhuis and Van Dijk, 2002). However, prey densities on migration routes to some breeding sites appear to be quite low compared to the wintering area (Feder et al., 1994; Lovvorn et al., 2009). Our observations in 2009 suggested that when wintering sites with adequate prey densities are covered with dense sea ice, spectacled eiders may have difficulty achieving sufficient reserves before spring migration and breeding.

The movement of nutrient rich water through the northern Bering Sea, the rate of deposition of chlorophyll to northern Bering Sea sediments, and mixing throughout the water column suggests an abundance of nutrient and planktonic resources for benthic bivalves, thereby supporting locally high densities of prey for eiders and other apex predators. However, intra-annual movement of eiders within the primary wintering area in response to sea ice concentration and flow suggested that in some winters ice may control the distribution of wintering eiders. Furthermore, eiders were observed roosting on the surface of sea ice adjacent to water during aerial surveys, suggesting that sea ice might also play a positive role in the winter ecology of the species. However, the ecology of spectacled eiders in the northern Bering Sea remains poorly understood. Unknown aspects include the frequency of foraging bouts, and the relative importance of sea ice as a barrier to food or as a platform for resting or heat conservation out of water.

4. Conclusions

Observations of hydrographic and biological conditions in March 2008, 2009, and 2010 indicated that the northern Bering Sea is biologically active during the late winter–early spring transition in part due to the presence of significant populations of apex predators, including almost the entire world population of spectacled eiders. Chlorophyll stocks in the water column however are relatively low, and fluxes are less on an areal basis than surface sediment inventories, suggesting seasonal accumulation of organic matter on the sea floor despite significant metabolic activity (e.g. oxygen respiration) in the sediments. Chlorophyll is concentrated on the bottom of the sea ice, and high nutrient concentrations throughout the water column and up to the surface sustain growth of these sea ice algal communities. West-to-east decreases in salinity, nutrients and water-column chlorophyll readily apparent in the open water season (e.g. Walsh et al., 1989) are muted at this time because biological production has not reached high enough levels to significantly impact inorganic nutrient or chlorophyll concentrations. Salinity variation is more influenced by brine injection than water mass differences, which is corroborated by the stable oxygen isotope data from surface waters. We also observed distributions of the stable isotope ^{18}O that suggest potential use of the isotope as a tracer of new ice production in polynyas.

Finally, we were able to document the interannual distribution of spectacled eiders within these waters, which are clearly important for this species due to the high concentrations of benthic foods. Aggregations of spectacled eiders were associated with open leads and high benthic food resources. However, eiders were forced into presumably less productive waters when sea ice precluded use of areas with greater benthic biomass. Therefore, the balance between food availability and abiotic variables, such as sea ice extent and lead formation, is a likely important controlling factor for eiders and other apex predators in the northern Bering Sea. In years of heavy ice cover, the spatiotemporal distribution of spectacled eiders within the primary wintering area appears to be controlled by the formation and movement of sea ice, in addition to sources of food as determined by biological productivity.

Acknowledgments

The field sampling would not have been possible without strong support from the commanding officers, crew and officers

of both the USCGC *Healy* on the 2008 and 2009 cruises, and during the apparently final science mission of the USCGC *Polar Sea* in 2010. Shipboard support for water column collections and data management was provided by Steve Roberts, Tom Bolmer, Matt Durham, Ben Gire, Sigrid Salo, Peter Proctor, Mark Bradford, John Allison, and Scott Hiller. Also at sea, we thank Markus Janout, Boris Sirenko, Craig Casemodel, Deanna Wheeler, Rebecca Neumann, Sarah Story, Joe Bump, Perry Pungowiyi, Gay Sheffield, Marisa Guarinello, Regan Simpson, Krista Hoff, Maria Ceballos, Linton Beaven, Cynthia Yeung, Laura Gemery, Nathalie Morata, Jared Weems, Brenna McConnell, Marjorie Brooks, Steve Fenske, Dawn Sechler, Martin Schuster, and Edward Davis for their help in collecting the data presented here. Alynne Bayard and Aariel Rowan provided GIS expertise with drafting some of the figures and Dana Biasatti made the oxygen isotope determinations. We thank two anonymous reviewers and guest editor Mike Lomas for their efforts in reviewing earlier versions of the manuscript. Financial support was provided in part by the North Pacific Research Board. The Office of Polar Programs of the National Science Foundation also supported this work, through ARC-0732767 to RG, ARC-0732430 to CM, and ARC-082290 to L.C. and J.G. The spectacled eider telemetry efforts were supported by the Bureau of Ocean Energy Management, the Bureau of Land Management, the National Fish and Wildlife Foundation, the US Fish and Wildlife Service, ConocoPhillips-Alaska, Inc., the Columbus Zoo and Aquarium, the Mesker Park Zoo & Botanic Garden, and the Point Defiance Zoo & Aquarium. Use of trade names is for descriptive purposes only and does not imply endorsement by the US Geological Survey or the US Government. This study was also in part funded by the Joint Institute for the Study of the Atmosphere and Ocean (JISAO) under NOAA Cooperative Agreement no. NA17RJ1232. This work is Contribution 3854 to NOAA's Pacific Environmental Laboratory, 2041 to JISAO, EcoFOCI-0786 to NOAA's Fisheries-Oceanography Coordinated Investigations, and Contribution 87 to the BEST-BSIERP program.

References

Arar, E.J., Collins, G.B., 1997. Method 445.0. In Vitro Determination of Chlorophyll *a* and Pheophytin *a* in Marine and Freshwater Algae by Fluorescence, Revision 1.2. National Exposure Research Laboratory Office of Research and Development U.S. Environmental Protection Agency Cincinnati, Cincinnati, OH 45268, p. 22.

Beyer, H.L., 2012. Geospatial Modelling Environment (Version 0.6.0.0). (software). URL: ⟨http://www.spatialecology.com/gme⟩.

Clement, J.L., Cooper, L.W., Grebmeier, J.M., 2004. Late winter water column and sea ice conditions in the northern Bering Sea. J. Geophys. Res. 109, C3), http://dx.doi.org/10.1029/2003JC002047, C03022.

Clement, J.L., Maslowski, W., Cooper, L.W., Grebmeier, J.M., Walczowski, W., 2005. Ocean circulation and exchanges through the northern Bering Sea—1979–2001 model results. Deep-Sea Res. II 52, 3509–3540.

Cooper, L.W., Whitledge, T.E., Grebmeier, J.M., Weingartner, T., 1997. The nutrient, salinity, and stable oxygen isotope composition of Bering and Chukchi Seas waters in and near the Bering Strait. J. Geophys. Res. 102, 12563–12573.

Cooper, L.W., Grebmeier, J.M., Larsen, I.L., Dolvin, S., Reed, A.J., 1998. Inventories and distribution of radiocessium in arctic marine sediments: influence of biological and physical processes. Chem. Ecol. 15, 27–46.

Cooper, L.W., Grebmeier, J.M., Larsen, I.L., Egorov, V.G., Theodorakis, C., Kelly, H.P., Lovvorn, J.R., 2002. Seasonal variation in sedimentation of organic materials in the St. Lawrence Island polynya region, Bering Sea. Mar. Ecol. Prog. Ser. 226, 13–26.

Cooper, L.W., Janout, M.A., Frey, K.E., Pirtle-Levy, R., Guarinello, M.L., Grebmeier, J.M., Lovvorn, J.R., 2012. The relationship between sea ice break-up, water mass variation, chlorophyll biomass, and sedimentation in the northern Bering Sea. Deep Sea Research Part II 65, 141–162, http://dx.doi.org/10.1016/j.dsr2.2012.02.002.

Coulson, J.C., 1984. The population dynamics of the eider duck *Somateria mollissima* and evidence of extensive non-breeding by adult ducks. Ibis 126, 525–543.

Danielson, S., Aagaard, K., Weingartner, T., Martin, S., Winsor, P., Gawarkiewicz, G., Quadfasel, D., 2006. The St. Lawrence polynya and the Bering shelf circulation: new observations and a model comparison. J. Geophys. Res. 111, C09023.

L Danielson, S., Eisner, L., Weingartner, T., Aagaard, K., 2011. Thermal and haline variability over the central Bering Sea shelf: Seasonal and interannual perspectives. Conti. Shelf Res 31 (6), 539–554.

Douglas, D., 2010. The Douglas Argos-Filter Algorithm, Version 7.03 (Software). USGS Alaska Science Center. Available at: ⟨http://alaska.usgs.gov/science/biology/spatial/douglas.html⟩.

Ely, C.R., Dau, C.P., Babcock, C.A., 1994. Decline in a Population of Spectacled Eiders Nesting on the Yukon-Kuskokwim Delta. Alaska. Northwestern Naturalist 75 (3), 81–87.

ESRI, 2010. ArcGIS Desktop: Release 10 (Software). Environmental Systems Research Institute, Redlands, CA.

Feder, H.M., Foster, N.R., Jewett, S.C., Weingartner, T.J., Baxter, R., 1994. Mollusks in the northeastern Chukchi Sea. Arctic 47, 145–163.

Gordon, L., Jennings, J., Ross, A., Krest, J., 1994. A Suggested Protocol for Continuous Flow Analysis of Seawater Nutrients (Phosphate, Nitrate, Nitrite, and Silicic Acid) in the WOCE Hydrographic Program and the Joint Global Ocean Fluxes Study. WHP Office Report.

Gradinger, R., Meiners, K., Plumley, G., Zhang, Q., Bluhm, B.A., 2005. Abundance and composition of the sea-ice meiofauna in off-shore pack ice of the Beaufort Gyre in summer 2002 and 2003. Polar Biol. 28, 171–181.

Grebmeier, J.M., 2012. Biological community shifts in Pacific Arctic and sub-Arctic seas. Ann. Rev. Mar. Sci. 4, 63–78 10.114/annurev-marine-120710-100926.

Grebmeier, J.M., McRoy, C.P., 1989. Pelagic–benthic coupling on the shelf of the northern Bering and Chukchi Seas. III. Benthic food supply and carbon cycling. Mar. Ecol.: Prog. Ser. 53, 79–91.

Grebmeier, J.M., Cooper, L.W., 1995. Influence of the St. Lawrence Island Polynya upon the Bering Sea Benthos. J. Geophys. Res. 100, 4439–4460.

Grebmeier, J.M., Cooper, L.W., Feder, H.M., Sirenko, B.I., 2006. Ecosystem dynamics of the Pacific influenced Northern Bering and Chukchi Seas. Prog. Oceanogr. 71, 331–361.

Grebmeier, J.M., Barry, J.P., 2007. Benthic processes in polynyas. In: W.O. Smith, Jr., D.G. Barber (Eds.), Polynyas: Windows to the World, Elsevier Oceanography Series, vol. 74, pp. 363–390.

Kanneworff, E., Nicolaisen, W., 1973. The "HAPS": a frame supported bottom corer. Ophelia Supplement 10, 119–129.

Kinder, T.H., Coachman, L.K., Galt, J.A., 1975. The Bering slope current system. J. Phys. Oceanogr. 5, 231–244.

Korschgen, C.E., Kenow, K.P., Gendron-Fitzpatrick, A., Green, W.L., Dein, F.J., 1996. Implanting intra-abdominal radiotransmitters with external whip antennas in ducks. J. Wildl. Manage. 60, 132–137.

Lovvorn, J.R., Richman, S.E., Grebmeier, J.M., Cooper, L.W., 2003. Diet and body condition of spectacled elders wintering in pack ice of the Bering Sea. Polar Biol. 26, 259–267.

Lovvorn, J.R., Grebmeier, J.M., Cooper, L.W., Bump, J.K., Richman, S.E., 2009. Modeling marine protected areas for threatened eiders in a climatically changing Bering Sea. Ecol. Appl. 19, 1596–1613.

Macdonald, R.W., McLaughlin, F.A., Wong, C.S., 1986. The storage of reactive silicate samples by freezing. Limnol. Oceanogr. 31, 1139–1142.

Michel, C., Ingram, R.G., Harris, L.R., 2006. Variability in oceanographic and ecological processes in the Canadian Arctic Archipelago. Prog. Oceanogr. 71, 379–401.

Mordy, C.W., Cokelet, E.D., Ladd, C., Menzia, F.A., Proctor, P., Stabeno, P.J., Wisegarver, E., 2012. Net community production on the middle shelf of the eastern Bering Sea. Deep-Sea Res. II 65–70, 110–125.

Mulcahy, D.M., Esler, D., 1999. Surgical and immediate postrelease mortality of Harlequin Ducks implanted with abdominal radio transmitters with percutaneous antennae. J. Zoo Wildlife Med. 30, 397–401.

Oosterhuis, R., Van Dijk, K., 2002. Effect of food shortage on the reproductive output of common eiders *Somateria mollissima* breeding at Griend (Wadden Sea). Atlantic Seabirds 4, 29–38.

Petersen, M.R., Larned, W.W., Douglas, D.C., 1999. At-sea distribution of Spectacled Eiders: a 120-year-old mystery resolved. Auk 116, 1009–1020.

Petersen, M.R., Grand, J.B., Dau, C.P., 2000. Spectacled eider (*Somateria fischeri*). In: Poole, A., Gill, F. (Eds.), The Birds of North America, No. 547. The Birds of North America, Inc., Philadelphia, PA.

Pirtle-Levy, R., Grebmeier, J.M., Cooper, L.W., Larsen, I.L., 2009. Seasonal variation of chlorophyll *a* in Arctic sediments implies long persistence of plant pigments. Deep-Sea Res. II 56, 1326–1338.

Stehn, R.A., Dau, C.P., Conant, R., Butler Jr., W.I., 1993. Decline of spectacled eiders nesting in western Alaska. Arctic 46, 264–277.

US Fish and Wildlife Service, 1993. Final rule to list the spectacled eider as threatened. Federal Register 58, 27374–27480.

U.S. Fish and Wildlife Service, 2001. Endangered and threatened wildlife and plants; final determination of critical habitat for the spectacled eider. Federal Register 66, 9146–9185.

Wang, J., Hu, H., Mizobata, K., Saitoh, S., 2009. Seasonal variations of sea ice and ocean circulation in the Bering Sea: a model-data fusion study. J. Geophys. Res. 14, C02011.

Walsh, J.J., McRoy, C.P., Coachman, L.K., Goering, J.J., Nihoul, J.J., Whitledge, T.E., Blackburn, T.H., Parker, P.L., Wirick, C.D., Shuert, P.G., Grebmeier, J.M., Springer, A.M., Tripp, R.D., Hansell, D.A., Djenidi, S., Deleersnijder, E., Henricksen, K., Lund, B.A., Andersen, P., Müller-Karger, F.E., Dean, K., 1989. Carbon and nitrogen cycling within the Bering/Chukchi Seas: source regions for organic matter effecting AOU demands of the Arctic Ocean. Prog. Oceanogr. 22, 277–359.

Welschmeyer, N.A., 1994. Fluorometric analysis of chlorophyll *a* in the presence of chlorophyll *b* and pheopigments. Limnol. Oceanogr. 39, 1985–1992.

Whitledge, T.E., Reeburgh, W.S., Walsh, J.J., 1986. Seasonal inorganic nitrogen distributions and dynamics in the southeastern Bering Sea. Conti. Shelf Res. 5, 109–132.